

# Leptoproduction of nucleons in the cumulative region

M.A.Braun, V.V.Vechernin

Dep. High-Energy physics, S.Petersburg University, 198904 S.Petersburg, Russia,  
and B.Vlahovic  
NCCU, Durham, USA

## Abstract

Leptoproduction of nucleons into the backward hemisphere on nuclear targets is studied at relativistic subasymptotic energies and momenta. Spins are neglected. The relativistic internucleon potential is extracted from the appropriate photoproduction data. Different production mechanisms are shown to work together and interfere. Calculations show that whenever rescattering is possible it gives the bulk of the contribution except at very high  $Q^2$ . The Weizsaecker-Williams approximation is found to generally reproduce only a small part of the total cross-section. Comparison with the data for  $A(e,e'p)$  reaction at  $E=2.4$  GeV shows a reasonable agreement.

## 1 Introduction

Production of particles off nuclei in the cumulative domain  $x > 1$  presents a great interest, since it is related to the nuclear structure at small distances, where one may expect formation of multi-quark states and even droplets of a cold quark-gluon plasma. Staying within the most conservative picture of the nucleus consisting of nucleons interacting with some potentials, cumulative particle production allows to study the high-momentum asymptotics of these potentials and, which is of especial importance, multi-nucleon forces, otherwise hidden due to the low probability for several nucleons to be located at the same point. Experimental data demonstrate that the rate of cumulative production is very weakly dependent on the initial energy, starting from several GeV's. This allows to study cumulative production at comparatively low energy facilities, provided their luminosity is high enough to observe cross-sections dramatically falling as  $x$  grows beyond the threshold  $x = 1$ .

There has never been shortage of theoretical models to describe cumulative production off nuclei. All proposed models can be roughly divided into three categories. The first (also in time) is to ascribe the production to the presence of states with a nuclear density much higher than on the average in the initial nucleus [1,2]. Interpretation of these states may be different: just several nucleons at the same point ("many-body correlations" [3]) or multi-quark states [4]). The second mechanism assumes that such high-density states are rather formed in the course of the collision ("compressed tube" models [5]). Finally one can assume that the high nuclear densities are irrelevant and the cumulative particles are produced as a result of simple rescattering [6].

Microscopic studies, both in the nucleon and quark pictures, have shown that in reality all three mechanisms work together in the cumulative production. Moreover their contributions interfere, so that the total rate is not just the sum of them [7]. It is of most importance

that the contribution from the rescattering depends differently on the target properties than the other two. This prevents simple estimates of the cross-sections on heavy nuclei based on those with only few nucleons, as suggested in [ 8 ]. Only at sufficiently high momentum transferred to the nucleus, of all contributions, only the first one remains, corresponding to the few-nucleon correlations or multi-quark states inside the nucleus. From the theoretical point of view, it is the most interesting part, since it reveals the inner structure of the nucleus at short distances. However to see it clearly against the background of other components, one has to select events with high enough  $Q^2$ , which drastically diminishes already small cross-sections. Also the exact values of  $Q^2$  at which one can neglect the contributions from other two mechanisms are not known *a priori*.

For this reason it is important to carry out calculations of cumulative production at finite  $Q^2$  which take into account all three above mentioned mechanisms. In this way one expects to obtain predictions for the inclusive cross-sections, integrated over all  $Q^2$ , and thus directly related to the bulk of experimental data. Moreover, studying the relative weight of the contributions at different  $Q^2$  one may determine the minimum  $Q^2$  value, starting from which rescattering and compressed tube contributions can be safely neglected.

In this paper we do these calculations in the framework of the nucleon degrees of freedom. Estimates have shown that this description gives reasonable results at  $x$  not too close to the cumulative threshold  $x = n$  for  $n$  nucleons which interact at close distance from each other, provided one uses the correct relativistic kinematics [ 3 ]. We limit ourselves with the cumulative region  $1 < x < 2$ , easiest from both experimental and theoretical points of view. In this region it is commonly assumed that one has to study hard interactions of only two nucleons inside the nucleus. Since inclusion of relativistic spins presents serious difficulties for nuclei with  $A > 2, 3$ , we simplify our approach by taking nucleons scalar. This approximation may certainly change results by a factor of order  $2 \div 3$ . However in the cumulative region as  $x$  grows from 1 to 2 the cross-sections fall by several orders of magnitude. On this scale a factor of order unity plays a secondary role. In any case there is no reason to expect that the results obtained with scalar nucleons will have a different  $x$ ,  $p_{\perp}^2$  and  $A$  dependence as compared to the full spinor case, and it is this dependence which is of primary theoretical interest.

The paper is organized as follows. In Section 2 we present our basic formulas for the structure function and solve the most difficult task of extracting the rescattering contribution. In Section 3 we discuss how to pass from the structure function to the production rates. Our final results are presented in Section 4. Section 5 contains some discussion and conclusions. Appendix is devoted to certain non-trivial details of numerical calculations.

## 2 Structure functions in the interval $1 < x < 2$

### 2.1 Cross-sections and kinematics

We shall be interested in the inclusive leptonproduction of nucleons on nuclear targets in the cumulative kinematical domain. However it will be convenient to start with a simpler reaction

$$e + A \rightarrow e + X. \quad (1)$$

Its cross-section can be expressed via nuclear structure functions in the standard manner

$$\frac{d\sigma}{dE' d\Omega'} = \sigma_{Mott} \frac{1}{4\pi M} \left( \frac{M^2}{qP} F_2(x, Q^2) + 2 \tan^2 \frac{\theta}{2} F_1(x, Q^2) \right), \quad (2)$$

where

$$\sigma_{Mott} = 4 \frac{\alpha_{em}^2}{Q^4} (E')^2 \cos^2 \frac{\theta}{2}. \quad (3)$$

In our normalization the structure functions are related to the imaginary part of the forward amplitude for the elastic  $\gamma^* - A$  scattering as

$$W_{\mu\nu} = \left( -g_{\mu\nu} + \frac{q_\mu q_\nu}{q^2} \right) F_1(x, Q^2) + \frac{1}{qP} \left( P_\mu - q_\mu \frac{qP}{q^2} \right) \left( P_\nu - q_\nu \frac{qP}{q^2} \right) F_2(x, Q^2), \quad (4)$$

where  $q$  and  $P = Ap$  are the momenta of the photon and nucleus and, as usual,

$$Q^2 = -q^2, \quad x = \frac{Q^2}{2qp}. \quad (5)$$

Note that we define  $x$  respective to  $\gamma^* + N$  scattering, so that

$$0 \leq x \leq A \quad (6)$$

The region  $x > 1$  is cumulative.

The standard way to find the structure functions from  $W_{\mu\nu}$  is to choose a coordinate system in which  $q_+ = q_y = p_\perp = 0$  ("theoretical"). Marking the components of vectors and tensors in this system with bars, one finds

$$F_1(x, Q^2) = \bar{W}_{yy}, \quad F_2(x, Q^2) = \frac{Q^2}{2Axp_+^2} \bar{W}_{++}. \quad (7)$$

We take the nucleon at rest:  $\mathbf{p} = 0$ . To study leptonproduction of cumulative nucleons we shall have to use another system ("lab") in which the incoming lepton with momentum  $l$  is moving along the  $z$ -axis in the opposite direction, so that neglecting its mass  $l_+ = 0$ . These two systems are related by a spatial rotation, which can be split into two ones. Starting from the lab. system, the first rotation is to put the  $y$ -component of  $\mathbf{q}$  (or  $\mathbf{l}'$ ) to zero. This is just a rotation in the  $xy$  plane by the azimuthal angle  $\phi$ :

$$q'_x = q_x \cos \phi + q_y \sin \phi, \quad q'_y = -q_x \sin \phi + q_y \cos \phi = 0, \quad q'_z = q_z. \quad (8)$$

The second rotation in  $xz$  plane is to put  $q_+ = 0$ , that is  $q_z = -q_0$ :

$$q''_z = q'_z \cos \phi_1 + q'_x \sin \phi_1 = -q_0, \quad q''_x = -q'_z \sin \phi_1 + q'_x \cos \phi_1. \quad (9)$$

The first relation determines the value of angle  $\phi_1$  through the given value of the transferred energy  $q_0 = E - E'$ :

$$\cos \phi_1 = \frac{1}{\mathbf{q}^2} (-q_0 q_z \pm Q q'_x). \quad (10)$$

The two signs correspond to the two possibilities of directing  $q_x$  parallel or antiparallel to the  $x$ -axis.

To find the inclusive cross-section for the leptonproduction of cumulative nucleons we shall integrate the cross-section (2) over  $E'$  and  $\Omega'$ , present both structure functions in (2) as integrals over intermediate particles and then lift the integration over the momenta of the observed nucleon. The only point to have in mind is that the structure function and the inclusive cross-section are to be calculated in different reference systems, theoretical and lab respectively. Since both  $Q^2$  and  $qp$  will vary in the resulting expression for the production rate, it will be more convenient to characterize the cumulative region directly in terms of the momentum  $p_1$  of the observed nucleon in the lab system. We shall discuss the corresponding kinematics in Section 3.

The method we use to find the cross-section for the inclusive leptonproduction of nucleons from the inclusive leptonproduction of leptons is discussed and justified in Appendix 1. There one can also find the expression for the double inclusive cross-section for the process in which both the lepton and cumulative nucleon are observed. This cross-section can be found from (2) only averaged over the azimuthal directions of the observed nucleon.

## 2.2 Hard interactions between two nucleons

In the interval  $n - 1 < x < n$  the incoming virtual photon has to interact with at least  $n$  nucleons. Since the cross-section results rapidly diminishing with the number of interacting nucleons, our first approximation will be to take into account only the interaction with  $n$  nucleons in this interval. Then at  $1 < x < 2$  the incoming photon is to interact with two and only two nucleons (approximation of "pair correlations" for the short-range part). The two interacting nucleons will generally have large momenta  $\mathbf{k}$  and  $\mathbf{q} - \mathbf{k}$ , whereas the rest intermediate particles will be slow. Their momenta will be of the order of the standard nuclear ones, to be neglected wherever possible. Separating the large momentum part from the low momentum one we can present the total contribution to the amplitude for the reaction  $\gamma^* + A \rightarrow N(p_1) + N(p_2) + X$  as a sum of four diagrams, shown in Fig. 1,  $a - d$ , where the thin lines represent slow nucleons, thick ones represent fast or highly virtual nucleons and thick dashed lines represent the interaction between the nucleons with high momentum transfer.

An important point is that the high-momentum part responsible for the production of the cumulative nucleons involves both short- and long-range distances in the nucleus, the latter corresponding to the rescattering contribution. Also to note is that the short-range contribution comes both from diagrams  $a$  and  $b$  and from diagrams  $c$  and  $d$ . The first pair of diagrams corresponds to the presence of the correlated pair inside the initial nucleus before the collision. Ideologically this is close to the "flucton" model, which was used to explain the cumulative phenomena immediately after their observation. The second pair of diagrams,  $c$  and  $d$ , correspond however to correlations created in the course of the collision. This is in line with mechanisms proposed in so-called "hot" models, like the "compressed tube model". As we observe, inspection of Feynman diagrams shows that in fact all different mechanisms proposed so far to explain the cumulative phenomena coexist simultaneously. Moreover, as we shall discover presently, their contributions to the cross-section are not added incoherently, but interfere, which leads to important cancellations. Our task will be to separate the long-range rescattering contribution, and to take into account the mentioned interference, which we shall do following [ 6 ].

The imaginary part of the forward scattering amplitude corresponding to Fig. 1 is given by

$$W_{\mu\nu} = \frac{1}{2} f^2(Q^2) \int \frac{d^3 p_1}{(2\pi)^3 2p_{10}} \frac{d^3 p_2}{(2\pi)^3 2p_{20}} \prod_{j=1}^2 \frac{d^4 k_j}{(2\pi)^4} \frac{d^4 k'_j}{(2\pi)^4} \\ (2\pi)^4 \delta^4(k_1 + k_2 - k'_1 - k'_2) (2\pi)^4 \delta(p_1 + p_2 - q - k_1 - k_2) H_\mu(H'_\nu)^* T(k_1, k_2 | k'_1, k'_2), \quad (11)$$

where the notations are clear from Fig. 1. In particular  $f(Q^2)$  is the effective nucleon form-factor; blob  $T$  which includes the propagators of the nucleons 1 and 2 describes the nuclear recoil particles.

Factors  $H$  and  $H'$  depending on  $k_j$  and  $k'_j$ ,  $j = 1, 2$  respectively, correspond to the high-momentum part of the amplitude. Their denominators in the virtual nucleon propagators in Fig. 1  $a$  and  $b$  are respectively

$$m^2 - (2p - p_1)^2, \quad \text{and} \quad m^2 - (p_1 - q)^2.$$

Obviously they cannot vanish, since a stable nucleus cannot decay into a real nucleon and some other particles. The denominator in Fig. 1  $c$  and  $d$  is

$$m^2 - (q + k_1)^2 = \left[ E(\mathbf{k}_1 + \mathbf{q}) - E(\mathbf{k}_2) + E(\mathbf{p}_1) + E(\mathbf{q} - \mathbf{p}_1 + \mathbf{k}_1 + \mathbf{k}_2) \right] \\ \left[ E(\mathbf{k}_1 + \mathbf{q}) + E(\mathbf{k}_2) - E(\mathbf{p}_1) - E(\mathbf{q} - \mathbf{p}_1 + \mathbf{k}_1 + \mathbf{k}_2) \right]. \quad (12)$$

The first factor is the difference between the initial and final energies in the decay

$$N(\mathbf{k}_2) \rightarrow \bar{N}(-\mathbf{k}_1 - \mathbf{q}) + N(\mathbf{p}_1) + N(\mathbf{q} - \mathbf{p}_1 + \mathbf{k}_1 + \mathbf{k}_2)]$$

and cannot vanish due to stability of the nucleon. For this reason we can drop small momenta  $k_{1,2}$  in it. The second factor is the difference between the initial and final energies in the rescattering

$$N(\mathbf{k}_1 + \mathbf{q}) + N(\mathbf{k}_2) \rightarrow N(\mathbf{p}_1) + N(\mathbf{q} - \mathbf{p}_1 + \mathbf{k}_1 + \mathbf{k}_2)$$

and evidently may vanish. Taking into account the smallness of momenta  $k_1$  and  $k_2$  we can rewrite it as

$$E(\mathbf{q}) + m - E(\mathbf{p}_1) - E(\mathbf{q} - \mathbf{p}_1) + \frac{\mathbf{k}_1 \mathbf{q}}{E(\mathbf{q})} - \frac{(\mathbf{k}_1 + \mathbf{k}_2, \mathbf{q} - \mathbf{p}_1)}{E(\mathbf{q} - \mathbf{p}_1)}. \quad (13)$$

So finally the denominator (12) takes the form

$$m^2 - (q + k_1)^2 = a(u + \alpha - i0), \quad (14)$$

where

$$a = E(\mathbf{q}) + E(\mathbf{p}_1) + E(\mathbf{q} - \mathbf{p}_1) - m, \quad (15)$$

$$u = E(\mathbf{q}) + m - E(\mathbf{p}_1) - E(\mathbf{q} - \mathbf{p}_1) \quad (16)$$

and

$$\alpha = \frac{\mathbf{k}_1 \mathbf{q}}{E(\mathbf{q})} - \frac{(\mathbf{k}_1 + \mathbf{k}_2, \mathbf{q} - \mathbf{p}_1)}{E(\mathbf{q} - \mathbf{p}_1)}. \quad (17)$$

Thus approximating  $k_1 = k_2 = p$  everywhere except in the denominator (14) we find the high-momentum factor as

$$H_\mu = K_\mu^{(a)} \frac{v(p_1 - p)}{m^2 - (2p - p_1)^2} + K_\mu^{(b)} \frac{v(p_1 - q - p)}{m^2 - (q - p_1)^2} + K_\mu^{(c)} \frac{v(p_1 - p) + v(p_1 - q - p)}{a(u + \alpha - i0)}. \quad (18)$$

We are only interested in  $+$  and  $y$  components of  $H$ . Factors  $K_+$  and  $K_y$  are identical for  $H$  and  $H'$  and in our system they are

$$K_+^{(a)} = 2(2p_+ - p_{1+}), \quad K_+^{(b)} = 2p_{1+}, \quad K_+^{(c)} = 2p_+ \quad (19)$$

and

$$K_y^{(a)} = -K_y^{(b)} = -2p_{1y}, \quad K_y^{(c)} = 0. \quad (20)$$

To move further we first integrate over the zero components of  $k_j$  and  $k'_j$ . The  $\delta$  functions which correspond to the conservation of energy have the form

$$\delta(k_{10} + k_{20} + P'_0 - P_0) \delta(k_{10} + k_{20} + P'_0 - P_0) \delta(p_{10} + p_{20} + P'_0 - q_0 - P_0). \quad (21)$$

Here  $P_0$  and  $P'_0$  are the energies of the target nucleus and its debris respectively. Using the first two  $\delta$ -function we integrate over the zero components of the two active nucleons 1 and 2. In coordinate space this integration puts both active nucleons at the same time. If we take into account only poles of their propagators and free nucleons for the debris, it produces the standard denominators of the wave function of the target nucleus.

Now we make the decisive approximation and neglect small energies of the nuclear debri as compared to fast particles in the last  $\delta$ -function in (21) taking it as

$$\delta(p_{10} + p_{20} - q_0 - 2m). \quad (22)$$

This allows to integrate blob  $T$  over the energy  $P'_0$  of the debri, which puts initial and final active nucleons at the same time point. As a result  $T$  transforms into the nuclear  $\rho$ -matrix for a pair of active nucleons:

$$\int \frac{dk_{20}}{2\pi} \frac{dk'_{20}}{2\pi} \frac{dP'_0}{2\pi} T(k_1, k_2 | k'_1, k'_2) = A(A-1) \rho(\mathbf{k}_1, \mathbf{k}_2 | \mathbf{k}'_1, \mathbf{k}'_2). \quad (23)$$

It is convenient to pass to the  $\rho$  matrix in the coordinate space presenting:

$$\begin{aligned} & (2\pi)^3 \delta^3(k_1 + k_2 - k'_1 - k'_2) \rho(\mathbf{k}_1, \mathbf{k}_2 | \mathbf{k}'_1, \mathbf{k}'_2) \\ &= \int \prod_{j=1}^2 d^3 r_j d^3 r'_j \rho(\mathbf{r}_1, \mathbf{r}_2 | \mathbf{r}'_1, \mathbf{r}'_2) e^{i(\mathbf{k}_1 \mathbf{r}_1 + \mathbf{k}_2 \mathbf{r}_2 - \mathbf{k}'_1 \mathbf{r}'_1 - \mathbf{k}'_2 \mathbf{r}'_2)} \end{aligned} \quad (24)$$

and write the imaginary part of the forward scattering amplitude in the form

$$\begin{aligned} W_{\mu\nu} &= \frac{1}{2} A(A-1) f^2(Q^2) \int d\tau \int \prod_{j=1}^2 \frac{d^3 k_j d^3 k'_j d^3 r_j d^3 r'_j}{(2\pi)^6} \\ &\quad \rho(\mathbf{r}_1, \mathbf{r}_2 | \mathbf{r}'_1, \mathbf{r}'_2) e^{i(\mathbf{k}_1 \mathbf{r}_1 + \mathbf{k}_2 \mathbf{r}_2 - \mathbf{k}'_1 \mathbf{r}'_1 - \mathbf{k}'_2 \mathbf{r}'_2)} H_\mu(H'_\nu)^*, \end{aligned} \quad (25)$$

where

$$d\tau = \frac{d^3 p_1}{(2\pi)^3 2p_{10}} \frac{d^3 p_2}{(2\pi)^3 2p_{20}} (2\pi)^4 \delta(p_1 + p_2 - q - 2p) \quad (26)$$

is the standard phase volume for the virtual photo-production on a pair of nucleons at rest.

### 2.3 Short and long range parts

We start with the component  $W_{yy}$ . As follows from (20) it does not contain any terms singular at  $k_j = k'_j = 0$ ,  $j = 1, 2$  and so can be taken at this point. Then integration over  $k_j$  and  $k'_j$ ,  $j = 1, 2$  gives four 3-dimensional  $\delta$ - functions which will put coordinates  $r_j = r'_j = 0$ ,  $j = 1, 2$ :

$$W_{yy} = \frac{1}{2} A(A-1) f^2(Q^2) \rho_0 \int d\tau H_y^2, \quad \rho_0 \equiv \rho(0, 0 | 0, 0). \quad (27)$$

Obviously this corresponds to a pure short range mechanism, both direct and spectator.

Passing to  $W_{++}$  we split  $H_+$  into parts singular and non-singular at  $k_j = 0$ ,  $j = 1, 2$

$$H_+ = \tilde{H}_+ + \frac{B}{u + \alpha - i0}, \quad (28)$$

where  $\tilde{H}_+$  is a non-singular part and according to (18)

$$B = 2p_+ \frac{v(p_1 - p) + v(p_1 - q - p)}{E(\mathbf{q}) + E(\mathbf{p}_1) + E(\mathbf{q} - \mathbf{p}_1) - m}. \quad (29)$$

Doing the same for  $(H'_+)^*$  we find

$$H_+(H'_+)^* = \tilde{H}_+^2 + 2B\tilde{H}_+\text{Re} \frac{1}{u-i0} + B^2 \frac{1}{u+\alpha-i0} \frac{1}{u+\alpha'+i0}, \quad (30)$$

where we have put  $k_j = k'_j = 0$ ,  $j = 1, 2$ , wherever possible.

The first two terms in (30) do not depend on  $k_j, k'_j$ ,  $j = 1, 2$  and so integration over these leads to a short-range contribution similar to (27)

$$\tilde{W}_{++} = \frac{1}{2}A(A-1)f^2(Q^2)\rho_0 \int d\tau \left( \tilde{H}_+^2 + 2B\tilde{H}_+\text{Re} \frac{1}{u-i0} \right). \quad (31)$$

To treat the singular contribution we first symmetrize it in primed and non-primed momenta

$$X \equiv \frac{1}{u+\alpha-i0} \frac{1}{u+\alpha'+i0} \rightarrow \frac{1}{2} \left( \frac{1}{u+\alpha-i0} \frac{1}{u+\alpha'+i0} + \frac{1}{u+\alpha+i0} \frac{1}{u+\alpha'-i0} \right).$$

Next we use

$$\frac{1}{u+\alpha-i0} = \frac{1}{u+\alpha+i0} + 2\pi\delta(u+\alpha)$$

to find

$$\begin{aligned} X &= \frac{1}{2} \left( \frac{1}{u+\alpha+i0} \frac{1}{u+\alpha'+i0} + 2\pi i\delta(u+\alpha) \frac{1}{u+\alpha'+i0} \right. \\ &\quad \left. + \frac{1}{u+\alpha-i0} \frac{1}{u+\alpha'-i0} - 2\pi i\delta(u+\alpha) \frac{1}{u+\alpha'-i0} \right) \\ &= \text{Re} \frac{1}{(u+\alpha-i0)(u+\alpha'-i0)} + 2\pi^2\delta(u+\alpha)\delta(u+\alpha'). \end{aligned} \quad (32)$$

The first term is non-singular at  $k_j = k'_j = 0$ ,  $j = 1, 2$  and can be rewritten as  $\text{Re} 1/(u-i0)^2$ . The second reduces to  $2\pi^2\delta(u)\delta(\alpha-\alpha')$ . Taking into account that  $k_1+k_2 = k'_1+k'_2$  we find that  $\alpha-\alpha' = (\mathbf{q}, \mathbf{k}_1 - \mathbf{k}'_1)/\mathbf{E}(\mathbf{q})$ , so that finally

$$X = \frac{1}{(u-i0)^2} + 2\pi^2 E(\mathbf{q})\delta(u)\delta(\mathbf{q}, \mathbf{k}_1 - \mathbf{k}'_1). \quad (33)$$

The first term in (33) does not depend on  $k_j = k'_j$ ,  $j = 1, 2$  and its integration is similar to the previous terms. It also corresponds to a short-range contribution and summing with (31) forms the complete short-range part of  $W_{++}$ :

$$W_{++}^{(s)} = \frac{1}{2}A(A-1)f^2(Q^2)\rho_0 \int d\tau \left( \tilde{H}_+^2 + 2B\tilde{H}_+\text{Re} \frac{1}{u-i0} + B^2\text{Re} \frac{1}{(u-i0)^2} \right). \quad (34)$$

The second term in (33) describes the long-range mechanism corresponding to real rescattering. It contains non-trivial dependence on small nuclear momenta. To do the integrations over  $k_j = k'_j$ ,  $j = 1, 2$  we direct  $\mathbf{q}$  along the  $z$ -axis. Then integrations over  $k_{1\perp}, k'_{1\perp}, k_2, k'_2$  and the corresponding coordinates are done as before and the only non-trivial integrations left are over  $k_{1z}$  and  $k'_{1z}$ . We find the long-range part of  $W_{++}$  as

$$W_{++}^{(l)} = \frac{1}{2}A(A-1) \int d\tau 2\pi^2 \frac{E(\mathbf{q})}{|\mathbf{q}|} B^2 \delta(u) \int \frac{dk_{1z}}{2\pi} dz_1 dz'_1 e^{ik_{1z}(z_1-z'_1)} \rho(0_\perp, z_1; 0|0_\perp, z'_1; 0)$$

$$= 2\pi^2 l \frac{E(\mathbf{q})}{|\mathbf{q}|} \int d\tau B^2 \delta(u), \quad (35)$$

where

$$l = \frac{1}{2} A(A-1) \int dz \rho(0_\perp, z; 0|0_\perp, z; 0) \quad (36)$$

has a meaning of the average dimension of the nucleus, travelled by the nucleon in rescattering. Note that due to energy conservation  $u$  and  $a$  can be rewritten as

$$u = E(\mathbf{q}) - q_0 - m, \quad a = E(\mathbf{q}) + q_0 + m \quad (37)$$

and do not depend on integration variables in (35). So one can take  $\delta(u)$  out of the integral (35). This leads to our final formula for the long-range contribution

$$W_{++}^{(l)} = 2\pi^2 l f^2(Q^2) \delta(E(\mathbf{q}) - q_0 - m) \frac{E(\mathbf{q})}{|\mathbf{q}|} \int d\tau B^2. \quad (38)$$

Note that it has a  $\delta$ -like behaviour in  $x$ . Indeed

$$\begin{aligned} \delta(E(\mathbf{q}) - q_0 - m) &= 2(q_0 + m) \delta(E^2(\mathbf{q}) - (q_0 + m)^2) \\ &= 2(q_0 + m) \delta(Q^2 - 2mq_0) = \delta(x - 1) \frac{Q^2 + 2m^2}{2mQ^2}. \end{aligned}$$

So in fact the rescattering does not give any contribution to the structure function in the cumulative region. However it does contribute to cumulative particle production.

Note finally that our nuclear  $\rho$ - matrix is defined in the relativistic normalization. Its relation to the non-relativistic one is given by

$$\rho = \frac{A}{2m} \rho_{NR}.$$

### 3 Cumulative nucleon production

We shall be interested in the observation of a nucleon of momentum  $p_1$  produced in the reaction

$$l + A \rightarrow N(p_1) + X, \quad (39)$$

where  $l$  is the incoming lepton of momentum  $l$  and  $A$  is the target nucleus at rest. We shall direct  $l$  antiparallel to the  $z$ -axis to have the system close to the theoretical system in which  $q_+ = 0$ . With such a choice non-cumulative nucleons will be produced in the *backward* hemisphere, whereas cumulative ones will be observed also in the forward hemisphere. The exact non-cumulative kinematical region in the lab. system can be easily established in light-cone variables, using the fact that in this system  $l_+ = 0$ . Let  $p_{1+} = x_1 p_+$ . Obviously in the non-cumulative region  $0 < x_1 < 1$ . Conservation of the "-" component of the momentum (light-cone energy) requires

$$l_- + p_- = p_{1-} + p'_-, \quad (40)$$

where  $p'$  is the momentum of the undetected particles. The minimal mass of the latter is zero. So in terms of initial energy  $E$  we get a relation

$$\frac{1}{\sqrt{2}}(2E + m) \geq \frac{m^2 + p_{1\perp}^2}{2x_1 p_+} + \frac{p_{1\perp}^2}{2(1 - x_1)p_+}, \quad (41)$$



which leads to the condition

$$p_{1\perp}^2 \leq x_1(1-x_1)m(2E+m) - (1-x_1)m^2 \quad (42)$$

Together with the relation between  $x_1, p_\perp$  and  $p_{1z}$ :

$$p_{1z} = \frac{1}{2}m \left( x_1 - \frac{m^2 + p_{1\perp}^2}{x_1 m^2} \right) \quad (43)$$

Eq. (42) determines the non-cumulative region in the  $p_{1z}, p_{1\perp}$  plane. The cumulative region for the pair correlation is determined by the corresponding energy conservation relation

$$l_- + 2p_- = p_- + p'_-, \quad (44)$$

where now the minimal mass of undetected particles equals  $m$ . In terms of  $x_1$  and  $p_{1\perp}$  this gives a relation

$$p_{1\perp}^2 = x_1(2-x_1)m(E+m) - m^2, \quad (45)$$

which together with (43) determines the cumulative region for the pair correlation. For the incident energy  $E = 6$  GeV in the backward hemisphere this region is limited by the solid line in Fig. 2 The dotted line limits the region corresponding to the rescattering discussed in the previous section.

As mentioned shall find the rate of cumulative nucleon production by using our results for the structure functions. Putting them into the integrated cross-section (2) we then lift the integration over the momentum  $p_1$  of the intermediate real nucleon. However we have to take into account that our expressions for the structure functions have been obtained in a special coordinate system  $q_+ = q_y = 0$  different from the lab. system for the reaction (1). This implies that we have to reexpress all momenta in the system  $q_+ = q_y = 0$  via the momenta in the lab. system.

Turning to our expressions for the structure functions, we see that in most places the vectors appear in the form of scalar products or invariant integration measures, which do not change under rotations. The only quantities which change their form under rotations are vectors  $K$ , in which we shall have to express the  $+$ - and  $y$ -components of vector  $p_1$  in the system  $q_+ = q_y = 0$  by its components in the lab.system:

$$p_{1y} \rightarrow \bar{p}_{1y} = -p_{1x} \sin \phi + p_{1y} \cos \phi, \quad p_{1z} \rightarrow \bar{p}_{1z} = p_{1z} \cos \phi_1 + (p_{1x} \cos \phi + p_{1y} \sin \phi) \sin \phi_1 \quad (46)$$

and keeping the same  $p_0$ .

Thus we get for the inclusive cross-section to observe a nucleon of momentum  $p_1$

$$\frac{(2\pi)^3 2p_{10} d\sigma}{d^3 p_1} = \int dE' d\Omega \sigma_{Mott} \frac{1}{4\pi M} \left( \frac{M^2}{qP} F_2(\mathbf{q}, \mathbf{p}_1) + 2 \tan^2 \frac{\theta}{2} F_1(\mathbf{q}, \mathbf{p}_1) \right). \quad (47)$$

Here the structure functions  $F_{1,2}(\mathbf{q}, \mathbf{p}_1)$  are obtained from the standard ones, calculated in the preceding section, by lifting the integration over  $p_1$ , that is discarding  $d^3 p_1 / ((2\pi)^3 2p_{10})$  in the integration volume  $dV$  in (34) and (38), and also changing  $p_{1y}$  and  $p_{1z}$  to  $\bar{p}_{1y}$  and  $\bar{p}_{1z}$  as indicated in (46). Note that angles  $\phi$  and  $\phi_1$  in the latter formulas depend on the remaining integration variables, related to the changing vector  $\mathbf{q} = \mathbf{l} - \mathbf{l}'$ .

Using (7) we rewrite (2) in terms of  $\bar{W}$ 's to obtain

$$\frac{(2\pi)^3 2p_{10} d\sigma}{d^3 p_1} = \frac{1}{4\pi A m} \int dE' d\Omega \sigma_{Mott} \left( \frac{m^2}{p_+^2} \bar{W}_{++}(q, p_1) + 2 \tan^2 \frac{\theta}{2} \bar{W}_{yy}(q, p_1) \right). \quad (48)$$

In  $W$ 's we have to lift the integration over  $\mathbf{p}_1$ . We rewrite the phase volume (26) in the form

$$d\tau = \frac{d^3 p_1}{(2\pi)^3 2p_{10}} \frac{d^4 p_2}{(2\pi)^4} 2\pi \delta(p_2^2 - m^2) (2\pi)^4 \delta^4(p_1 + p_2 - q - 2p)$$

and integrating over  $p_2$  find

$$d\tau = \frac{d^3 p_1}{(2\pi)^3 2p_{10}} 2\pi \delta((2p + q - p_1)^2 - m^2), \quad (49)$$

so that lifting the integration over  $\mathbf{p}_1$  substitutes

$$d\tau \rightarrow 2\pi \delta((2p + q - p_1)^2 - m^2). \quad (50)$$

In variables  $E', \theta, \phi$  we have

$$q_0 = E - E', \quad q_z = -E + E' \cos \theta, \quad q_x = -E' \sin \theta \cos \phi, \quad q_y = -E' \sin \theta \sin \phi, \quad (51)$$

$$Q^2 = 2EE'(1 - \cos \theta).$$

The fixed momentum  $\mathbf{p}_1$  can always be placed in the  $xz$  plane, so that  $p_{1y} = 0$ . The argument of the  $\delta$ -function in (49) turns out to be

$$(2p + q - p_1)^2 - m^2 = 4m^2 - Q^2 + 4pq - 4pp_1 - 2qp_1 = 2(b - E'\lambda(\theta, \phi)), \quad (52)$$

where

$$\lambda = E(1 - \cos \theta) + 2m - E_1 - p_{1z} \cos \theta + p_{1x} \sin \theta \cos \phi \quad (53)$$

and

$$b = 2m(m + E - E_1) - E(E_1 + p_{1z}). \quad (54)$$

Here  $E_1 = \sqrt{m^2 + p_{1z}^2 + p_{1x}^2}$  is the energy of the observed nucleon. Integrating this function we fix  $E'(\theta, \phi)$  and obtain an extra factor  $1/(2\lambda)$ . Thus we get

$$\frac{(2\pi)^3 2p_{10} d\sigma}{d^3 p_1} = \frac{1}{4Am} \int \frac{d \cos \theta d\phi}{\lambda(\theta, \phi)} \sigma_{Mott} \left( \frac{m^2}{p_+^2} \bar{W}_{++}(q, p_1) + 2 \tan^2 \frac{\theta}{2} \bar{W}_{yy}(q, p_1) \right), \quad (55)$$

where it is understood that we have to drop  $d\tau$  in  $W$ 's, make the substitutions (46) and express  $E'$  in terms of  $\theta$  and  $\phi$  using (52):

$$E' = b/\lambda(\theta, \phi). \quad (56)$$

Both  $b$  and  $\lambda(\theta, \phi)$  result positive and do not vanish in the integration region. However  $\sigma_{Mott}$  contains denominator  $Q^4$  typical for virtual-photon-mediated processes and leading to a logarithmic divergence for massless leptons  $m_l = 0$ . To cure this divergence we take in (55) the expression for  $Q^2$  for non-zero  $m_l$ :

$$Q^2 = 2EE' - 2\sqrt{(E^2 - m_l^2)(E'^2 - m_l^2)} \cos \theta - 2m_l^2. \quad (57)$$

Note that the standard Weiszaecker-Williams approximation takes into account only the leading term in  $\log(1/m_l)$  and thus expresses the cross-section via the real photoproduction. However calculations show that the Weiszaecker-Williams contribution is generally quite a small part of the total cross-section due to the fact that the amplitude vanishes at  $Q^2 = 0$ . This implies that leptoproduction cross-sections cannot be directly reduced to photoproduction ones.

Lifting one or both integrations in (55) and introducing appropriate phase volume factors one obtains cross-sections with  $Q^2$  or 4-vector  $q$  fixed respectively, averaged over the azimuthal directions of the observed nucleon. If one is interested also in this azimuthal dependence, one should use the formula for the double inclusive cross-section derived in Appendix 1.

## 4 Photoproduction of cumulative protons and the choice of the potentials

Expressions for  $H$  contain the relativistic potential  $v(k)$  which describes the pair interaction between the nucleons. A variety of relativistic potentials have been proposed which correctly describe the nucleon-nucleon scattering data at moderate energies. However, on the one hand, we actually need the high-energy asymptotics of the potential, which is fixed by these data not well enough. On the other hand, the proposed potentials refer to relativistic nucleons with spins and it is not clear how they can be used in our spinless picture. For this reason we shall recur to a different approach. We shall use the fact that for the process of the production of cumulative protons by real photons, the cross-sections are directly related to the internucleon potential. Therefore staying in the spinless picture and using the experimental data on the photoproduction on deuterium one can extract an effective internucleon potential as a function of the momentum transfer in a straightforward manner. However the energy dependence of this potential cannot be determined from the data, since the extracted potential refers to the energies close to the threshold. We studied two possibilities: an energy independent potential, similar to the exchange of scalar mesons, and a potential which grows with energy like the exchange of vectors mesons. Note that from a purely theoretical point of view the first alternative seems preferable, since it leads to vanishing of finite state interactions at high  $Q^2$  in correspondence with colour transparency following from the QCD. Also, as we shall see, our numerical results with the energy independent potential agree quite satisfactorily with the existing data on cumulative nucleon production, whereas with the vector-like potential they overshoot the data by factor 2.5 (see Fig. 11 below). For these reasons, we discuss below only the extraction from the photoproduction of an energy independent potential.

For unpolarized photons the total cross-section is

$$\sigma^{tot} = \frac{1}{J} e^2 \sum_{pol} e^\mu e^\nu W_{\mu\nu}, \quad (58)$$

where  $J = 4Apq$  is the invariant flux,  $e^\mu$  is the photon polarization vector and  $W_{\mu\nu}$  are the same as in Section 2.

We direct the momentum of the coming photon along the  $z$  axis. The integrand for  $W_{\mu\nu}$  involves a product  $H_\mu H'_\nu^*$  so that summing over polarization we get  $(eH)(eH)^* = H(H')_\perp^*$ . From (18) we find that diagrams  $c$  and  $d$  do not contribute to the cross-section in our approximation. Assuming that at  $Q^2 = 0$  only the proton interacts with the incoming photon, we are left with diagram  $b$  only (the direct mechanism) for which

$$H_\perp = 2p_{1\perp} \frac{v(p_1 - q - p)}{2qp_1}. \quad (59)$$

This obviously implies that there is no rescattering and we can safely drop small nuclear momenta in  $H$ . Repeating our derivation in Section 2 we find the total cross-section as

$$\sigma^{tot} = \frac{1}{2} (A-1) \rho_0 \frac{e^2}{8pq} \int d\tau H_\perp^2. \quad (60)$$

Passing to the inclusive cross-section for the production of a proton we make the substitution (50) to find

$$\frac{(2\pi)^3 2p_{10} d^3\sigma}{d^3p_1} = \frac{1}{2} (A-1) \rho_0 \frac{e^2}{8pq} 2\pi \delta((2p + q - p_1)^2 - m^2) H_\perp^2. \quad (61)$$

We shall use the lab system where the nucleus is at rest. Then  $qp = mE$  where  $E$  is the photon energy. The argument of the  $\delta$ -function in (61) is  $t + 4mE - 4mE_1 + 3m^2$ , where

$$t = (q - p_1)^2 = m^2 - 2E(E_1 - p_1 \cos \theta). \quad (62)$$

$E_1$  is the proton energy and  $\theta$  the angle between the proton and photon directions.

Transforming the phase volume element to variables  $t, E_1$  and using the  $\delta$  function to integrate over  $E_1$  we find

$$\frac{d\sigma}{dt} = \frac{1}{2}(A - 1)\rho_0 \frac{e^2}{256\pi m^2 E^2} H_\perp^2. \quad (63)$$

Note that in  $H_\perp$  the argument of the potential is

$$(p_1 - q - p)^2 = t + m^2 + 2m(E - E_1) = (1/2)(t - m^2) \equiv (1/2)t_1$$

and the denominator is  $2qp_1 = -t_1$ , so that we finally obtain

$$\frac{d\sigma}{dt} = \frac{1}{2}(A - 1)\rho_0 \frac{e^2 p_{1\perp}^2}{64\pi m^2 E^2} \left( \frac{v(t_1/2)}{t_1} \right)^2. \quad (64)$$

For the deuteron we have to substitute

$$\frac{1}{2}A(A - 1)\rho_0 = (1/m)\psi^2(0), \quad (65)$$

where  $\psi(r)$  is the deuteron wave function in the coordinate space.

As we observe, the photoproduction cross-section reveals a great simplicity in our approach: due to kinematical reasons the rescattering is absent and the cross-section becomes directly related to the high-momentum asymptotics of the effective internucleon potential. Therefore it is most suitable for studying this asymptotics. Of course one has to remember that our formulas may pretend to be valid only for the values of  $x$  sufficiently higher than unity. This is achieved in the emission of protons in the backward hemisphere relative to the direction of the incoming photon. Present data mostly refer to forward directions. Only the data [ 9 ] on the deuteron at the incident photon energy 4.0 GeV and  $\theta_1 = 90^\circ$  involve sufficiently high values of  $x$ . These data show that with more or less standard nuclear potentials borrowed from low energy physics one cannot describe the experiment above  $E = 1$  GeV. The experimental data for  $s^{11}d\sigma/dt$  show a clear plateau above 1.4 GeV in accordance with the QCD scaling law, whereas the predictions from the meson-exchange potentials steadily rise [ 9 ]. This is not at all unexpected, since one cannot hope that the relatively low energy parametrizations for the potential will work sufficiently well at high momentum transfers involved.

As mentioned, we are going to use the relation between the photoproduction cross-section and potential in the opposite direction. We determine the asymptotics of the effective nuclear potential from Eq. (64) putting the experimental data from [ 9 ] into its left-hand side. The latter can be satisfactorily fit by the expression

$$s^{11} \frac{d\sigma}{dt} (kbn * GeV^{20}) = 0.4 + 0.147741e^{-E^2} + 1.47116e^{-2E^2} \quad (66)$$

valid for  $E = 0.2 \div 4.0$  GeV. We take the value for the deuteron wave function at the origin as

$$\psi(0) = 3.131 \cdot 10^{-2} \text{GeV}^{3/2}.$$

The momentum space potential extracted in this manner is shown in Fig. 3. Compared to standard internucleon potentials it falls more rapidly with the transferred momentum. This is in agreement with the reduced nuclear amplitude approach of [ 10 ], in which hard exchanges between nucleons are to be accompanied by damping form-factors.

## 5 Numerical results

Using the effective potential extracted from the photoproduction data we calculated the leptonproduction cross-sections (55) for the initial lepton energy 6 GeV in the backward hemisphere on various nuclear targets. The  $A$  dependence of our cross-sections is concentrated in factors  $\rho_0$  and  $l$  for short- and long-range contributions correspondingly. These factors were calculated in the standard manner, neglecting correlations in the nuclear  $\rho$ -matrix and using the Woods-Saxon nuclear density. One finds

$$(A-1)\rho_0 = \frac{1}{2m}A(A-1) \int d^3r \rho_{NR}^2(r) \equiv m^2 f_0, \quad (67)$$

$$\frac{2}{A}l = \frac{1}{2m}A(A-1) \int d^2b T^2(b) \equiv mc_0. \quad (68)$$

Calculated dimensionless  $f_0$  and  $c_0$  are shown in Fig. 4 for different nuclei.

Numerical integrations in (55) encounter certain difficulties related to the singularities of the integrand at  $Q^2 = 0$  and the values of angle  $\theta$  limiting the rescattering region. Some details on this point are given in the Appendix 2.

Our results for the inclusive cross-section are presented in Figs. 5 and 6 for Cu and Pb targets for various angles in the backward hemisphere.

To see the relative importance of different production mechanisms, in Figs. 7-10 we show differential cross-sections in both  $\mathbf{p}_1$  and  $Q^2$  at  $Q^2 = 1$  and 4 (GeV/c)<sup>2</sup> and 90° and 180° on the Pb target. Solid curves correspond to the total contribution. Dashed and dash-dotted curves show contributions from the spectator mechanism and rescattering correspondingly.

As a general result we find that for the studied values of  $Q^2$  in the kinematical region where rescattering is possible it either completely dominates (at  $Q^2 \sim 1$  (GeV/c)<sup>2</sup> or lower) or gives a contribution of the same order as the spectator mechanism. The contribution of the direct mechanism has been always found quite small. At comparatively low values of  $Q^2$  the short range contribution from the final interaction ("compressed tube" mechanism) is also of the same order as the spectator mechanism and negative (see Fig. 8). However with the growth of  $Q^2$  its relative weight diminishes, as expected (cf. Fig. 10). We have also found that the relative contribution from the Weizsaecker-Williams term (leading in  $\log(1/m_l)$ ) is generally quite small, except at highest values of  $p_1$  for a given angle where it becomes of the same order or even several times larger than the rest short-range contribution.

To have some contact with existing experimental data on A(e,e'p) reaction we also calculated the double inclusive cross section  $d\sigma/(dE'd\Omega d\Omega_1)$  on the <sup>16</sup>O target, where  $\Omega$  and  $\Omega_1$  are angular variables for the final lepton and nucleon respectively. We have taken  $E = 2.4$  GeV,  $Q^2 = 0.8$  (GeV/c)<sup>2</sup> and  $q_0 = 0.439$  GeV corresponding to the experimental kinematics in [ 11 ]. Our results for the backward hemisphere are shown in Fig. 11 together with experimental points for the protons knocked out of 1p<sub>1/2</sub> shell (lower points) and 1p<sub>3/2</sub> shell (upper points). The recoil nucleon momenta result small in this kinematics, so that our approximation of neglecting the binding does not seem to be well justified. However the agreement is unexpectedly good: our calculated cross-sections well correspond to the experimental ones averaged over the two nuclear levels.

## 6 Conclusions

We have studied leptonproduction of cumulative nucleons on nuclear targets in a realistic subasymptotic kinematics, where all proposed mechanisms work together and interfere. Our results show that in the kinematical region where rescattering is possible, its contribution cannot be neglected unless  $Q^2$  is fixed and large. For the inclusive cross-section intergrated

over  $Q^2$  rescattering dominates the cross-section in this region. Of the rest mechanisms the direct one has been found to be completely unimportant at  $Q^2 > 1$  (GeV/c)<sup>2</sup>. However at smaller  $Q^2$  its contribution interferes with the rest mechanisms to make the amplitude vanish at  $Q^2 = 0$ . The short range part of the final state interaction (the compressed tube mechanism) gives a negative contribution, of the same order that the spectator contribution, except at high values of  $Q^2$  when it diminishes.

So, on the one hand, our results confirm the standard expectations that at very high  $Q^2$  only the spectator mechanism survives, which allows to simply relate the cumulative production on different nuclear targets [ 8 ]. On the other hand, they show that for realistic not too large  $Q^2$  and certainly for the inclusive cross-sections integrated over all  $Q^2$  all mechanisms give contributions of comparable order and interfere. In particular, in the kinematical region accessible for rescattering the latter gives a sizable (or even dominating) part of the contribution, which prevents using simple scaling arguments to fix the  $A$ -dependence.

Another important result is that the Weizsaecker-Williams approximation generally constitutes only a small part of the total cross-section. Thus leptonproduction cross-sections cannot be simply reduced to photoproduction ones.

Our calculations have been based on a simplified picture, in which all spins have been neglected. Accordingly the effective internucleon relativistic potential have been taken from the experimental photoproduction cross-sections, calculated within the same spinless approach. Comparison with the existing data on  $A(e,e'p)$  reaction reveals a reasonable agreement, which supports validity of our treatment.

## 7 Acknowledgements

M.A.B. is deeply thankful to the NCCU NC for hospitality and attention. This study was partially supported by the grant RFFI (Russia) 01-02-17137

## 8 Appendix 1. The double inclusive cross-section

In principle lifting integrations in the inclusive cross-sections does not give the exclusive ones: one can add any function to the thus obtained cross-section which integrates out to zero in the inclusive cross-section. So to have the double cross-section for the process in which both the lepton and nucleon are observed we have to study the amplitudes as they are, not via the inclusive form with the structure functions  $F_{1,2}$ . In our case this is possible (since the amplitudes are known).

The starting point is the basic formula for the cross-section

$$d\sigma = \frac{1}{4(Pl)} \frac{e^4}{q^4} L^{\mu\nu} W_{\mu\nu} d\tau \quad (69)$$

in which  $4Pl$  is the flux,  $L$  and  $W$  are the leptonic and hadronic tensors and  $d\tau$  is the phase volume. The leptonic tensor is

$$L_{\mu\nu} = \frac{1}{2} \sum_{pol} (\bar{u}' \gamma_\mu u) (\bar{u} \gamma_\nu u') = 2(l'_\mu l_\nu + l_\mu l'_\nu - (ll') g_{\mu\nu}). \quad (70)$$

The hadronic tensor can be represented by a symbolic product of two currents  $J$  which are in fact matrix elements of electromagnetic current between the initial and final hadronic states:

$$W_{\mu\nu} = J_\mu J_\nu^*. \quad (71)$$

Thus the cross-sections has the form

$$d\sigma = \frac{1}{2(Pl)} \frac{e^4}{q^4} d\tau \left[ (l'J)(lJ)^* + (lJ)(l'J)^* - (ll')(JJ^*) \right]. \quad (72)$$

We choose the system  $l_+ = l_- = 0$ . Then both the numerator and denominator become proportional to  $l_-$ , which cancels out. We get

$$\begin{aligned} d\sigma &= \frac{1}{2P_+} \frac{e^4}{q^4} d\tau \left[ (l'J)J_+^* + J_+(l'J)^* - l'_+(JJ^*) \right] \\ &= \frac{1}{2P_+} \frac{e^4}{q^4} d\tau \left[ (2l'_-J_+J_+^* + l'_+(JJ^*)_{\perp} - (l'J)_{\perp}J_+^* - J_+(l'J)_{\perp}^* \right]. \end{aligned} \quad (73)$$

Now we use that

$$l'_+ = \frac{1}{\sqrt{2}} E' (1 - \cos \theta) = \sqrt{2} E' \sin^2 \frac{\theta}{2}, \quad l'_- = \frac{1}{\sqrt{2}} E' (1 + \cos \theta) = \sqrt{2} E' \cos^2 \frac{\theta}{2}. \quad (74)$$

We also direct  $q_T$  along the  $x$ -axis, so that

$$l'_x = -E' \sin \theta. \quad (75)$$

The cross-section becomes

$$\begin{aligned} d\sigma &= \frac{1}{2P_+} \frac{e^4}{q^4} \sqrt{2} E' \cos^2 \frac{\theta}{2} d\tau \left[ (2J_+J_+^* + \tan^2 \frac{\theta}{2} (JJ^*)_{\perp} + \sqrt{2} \tan \frac{\theta}{2} (J_xJ_+^* + J_+J_x^*)) \right] \\ &= \frac{1}{2P_+} \frac{e^4}{q^4} \sqrt{2} E' \cos^2 \frac{\theta}{2} d\tau \left[ (|\sqrt{2}J_+ + \tan \frac{\theta}{2} J_x|^2 + \tan^2 \frac{\theta}{2} |J_y|^2) \right]. \end{aligned} \quad (76)$$

The first factor in (76) is

$$\frac{1}{2P_+} \frac{e^4}{q^4} \sqrt{2} E' \cos^2 \frac{\theta}{2} = \frac{4\pi^2}{ME'} \sigma_{Mott}. \quad (77)$$

We present

$$d\tau = \frac{d^3l'}{(2\pi)^3 2E'} d\tau_h, \quad (78)$$

where  $d\tau_h$  is the phase volume of the observed hadron. Then we finally get the exclusive cross-section as

$$d\sigma = dE' d\Omega' d\tau_h \frac{\sigma_{Mott}}{4\pi M} \left[ (|\sqrt{2}J_+ + \tan \frac{\theta}{2} J_x|^2 + \tan^2 \frac{\theta}{2} |J_y|^2) \right]. \quad (79)$$

To compare with the cross-section which is found by lifting the integrations in the inclusive cross-section we transform (79) to the system  $q_T = 0$ . This is achieved by a rotation in  $xz$  plane by angle  $\theta_0$  determined by

$$\tan \theta_0 = -\frac{q_x}{q_z} = \frac{E' \sin \theta}{E - E' \cos \theta}. \quad (80)$$

We find

$$d\sigma = dE' d\Omega' d\tau_h \frac{\sigma_{Mott}}{4\pi M} \left[ (|Z|^2 + \tan^2 \frac{\theta}{2} |J_y|^2) \right], \quad (81)$$

where now

$$Z = c_+ J_+ + c_- J_- + c_x J_x \quad (82)$$

with

$$c_{\pm} = \frac{1}{\sqrt{2}} \left( 1 \pm \cos \theta_0 \mp \sin \theta_0 \tan \frac{\theta}{2} \right), \quad c_x = \sin \theta_0 + \cos \theta_0 \tan \frac{\theta}{2}. \quad (83)$$

On the other hand, starting from the inclusive cross-section (2), dropping the integration over  $d\tau_h$  and passing from the system  $q_+ = 0$  to the system  $q_T = 0$  we obtain

$$d\tilde{\sigma} = dE' d\Omega' d\tau_h \frac{\sigma_{Mott}}{4\pi M} \left[ (|\tilde{Z}|^2 + 2 \tan^2 \frac{\theta}{2} |J_y|^2) \right] \quad (84)$$

with

$$\tilde{Z} = \tilde{c}_+ J_+ + \tilde{c}_- J_- + \tilde{c}_x J_x, \quad (85)$$

where

$$\tilde{c}_{\pm} = \frac{1}{\sqrt{2}} (1 \pm \cos \phi_0), \quad \tilde{c}_x = \sin \phi_0 \quad (86)$$

and

$$\tan \phi_0 = \frac{xM}{Q}. \quad (87)$$

One can trivially prove that

$$\cos \phi_0 = \cos \theta_0 - \sin \theta_0 \tan \frac{\theta}{2}, \quad \sin^2 \phi_0 + \tan^2 \frac{\theta}{2} = \left( \sin \theta_0 + \cos \theta_0 \tan \frac{\theta}{2} \right)^2. \quad (88)$$

So it turns out that

$$\tilde{c}_{\pm} = c_{\pm}, \quad \tilde{c}_x = \sqrt{c_x^2 - \tan^2 \frac{\theta}{2}}. \quad (89)$$

Comparing the correct cross-section (81) with the one (84) found from the inclusive cross-section, we see that they do not coincide, due to the difference in  $c_x$  and  $\tilde{c}_x$ . However if we integrate over the azimuthal directions of the observed nucleon, then both  $|J_x|^2$  and  $|J_y|^2$  go over to  $(1/2)|J_{\perp}|^2$  and the interference term with  $J_+ J_x^*$  vanishes. Then both cross-sections (81) and (84) give the same result.

Thus for the cross-sections averaged over the azimuthal directions of the observed nucleon one can use the inclusive cross-section with the dropped intergration over  $p_{1z}$  and  $p_{1\perp}$ . However if one wants to study also the azimuthal dependence, then one has to use the correct expression (81).

## 9 Appendix 2. Some calculational details

### 9.1 Singularity at $\theta = 0$

We present the cross-section (55) in the form

$$\frac{(2\pi)^3 2p_{10} d\sigma}{d^3 p_1} = \frac{\alpha_{em}^2}{4AmE^2} \int \frac{d\cos \theta d\phi}{(1 - \cos \theta)^2} X(\theta, \phi), \quad (90)$$



where

$$X(\theta, \phi) = \frac{\cos^2(\theta/2)}{\lambda(\theta, \phi)} \left( 2\bar{W}_{++}(q, p_1) + \tan^2 \frac{\theta}{2} \bar{W}_{yy}(q, p_1) \right). \quad (91)$$

With a zero lepton mass, the integral (90) diverges logarithmically at  $\theta = 0$  (corresponding to  $Q^2 = 0$ , a real photon). With a non-zero lepton mass  $m_l$  the divergence disappears, but the integrand still results strongly peaked at  $\theta = 0$ . To make its numerical calculation feasible one has naturally to separate the peak from the background.

Presenting at small  $\theta$

$$X(\theta, \phi) = \frac{1}{2}\theta^2 X_1(\phi) = (1 - \cos \theta)X_1(\phi) + \left( \cos \theta - 1 + \frac{1}{2}\theta^2 \right) X_1(\phi), \quad (92)$$

we write the integral (90) in the form

$$\frac{(2\pi)^3 2p_{10} d\sigma}{d^3 p_1} = \frac{\alpha_{em}^2}{4AmE^2} \int d\cos \theta d\phi \left[ \frac{(1 - \cos \theta)X_1(\phi)}{(1 - \cos \theta + \mu^2)^2} + \frac{X(\theta, \phi) - (1 - \cos \theta)X_1(\phi)}{(1 - \cos \theta)^2} \right], \quad (93)$$

where

$$\mu = \frac{m_l}{\sqrt{2}} \left( \frac{1}{E} + \frac{1}{E'} \right).$$

In the first term the integrations over  $\theta$  and  $\phi$  can be done explicitly. The result corresponds to the Weizsaecker-Williams approximation. From our study it follows that the dependence of  $X_1(\phi)$  on the azimuthal angle is trivial

$$X_1(\phi) = \cos^2 \phi X_{10}^{(1)} + \sin^2 \phi X_{10}^{(2)}, \quad (94)$$

where terms with *cos* and *sin* come from  $W_{++}$  and  $W_{yy}$  respectively. So the integration over  $\phi$  leads to the substitution

$$X_1(\phi) \rightarrow \pi(X_{10}^{(1)} + X_{10}^{(2)}) = \pi X_{10} \quad (95)$$

Integrating over  $\cos \theta$  we finally get

$$\frac{(2\pi)^3 2p_{10} d\sigma}{d^3 p_1} = \frac{(2\pi)^3 2p_{10} d\sigma^{WW}}{d^3 p_1} + \frac{\alpha_{em}^2}{4AmE^2} \int d\cos \theta d\phi \frac{X(\theta, \phi) - (1 - \cos \theta)X_1(\phi)}{(1 - \cos \theta)^2}, \quad (96)$$

where the Weizsaecker-Williams term is given by

$$\frac{(2\pi)^3 2p_{10} d\sigma^{WW}}{d^3 p_1} = \frac{\pi \alpha_{em}^2}{4AmE^2} X_{10} \left( \ln \frac{2}{\mu^2} - 1 \right). \quad (97)$$

The integration over  $\theta$  and  $\phi$  in the second term in (96) can only be done numerically.

## 9.2 Singularities of the short-range part of $X$

In the rescattering region the calculation of the short-range contribution to the integral (96) encounters difficulties generated by the singularities of  $\text{Re } H_+^2$  at  $(q + p)^2 = m^2$ . Denote

$$X_r(\theta, \phi) = X(\theta, \phi) - (1 - \cos \theta)X_1(\phi).$$

As a function of  $\phi$   $X_r$  has poles of the 1st and 2nd order in  $\cos \phi$ :

$$X_r(\theta, \phi) = X_{rr}(\theta\phi) + \frac{r_1(\theta)}{A(\theta) - B(\theta) \cos \phi} + \frac{r_2(\theta)}{(A(\theta) - B(\theta) \cos \phi)^2}, \quad (98)$$

where  $X_{rr}$  is a regular function. The poles exist only in a certain interval of  $\theta$

$$\theta_{min} < \theta < \theta_{max} \quad (99)$$

determined by the condition

$$\left| \frac{A(\theta)}{B(\theta)} \right| < 1, \quad (100)$$

where rescattering is kinematically possible.

Integration of  $\text{Re } X_r$  over  $\phi$  evidently gives

$$\int d\phi \text{Re } X_r(\theta, \phi) = \int d\phi \text{Re } X_{rr}(\theta, \phi), \quad (101)$$

for  $\theta$  inside the rescattering interval (99), and

$$\int d\phi \text{Re } X_r(\theta, \phi) = \int d\phi \text{Re } X_{rr}(\theta, \phi) + 2\pi \left( \frac{1}{\sqrt{A(\theta)^2 - B(\theta)^2}} + \frac{B(\theta)}{[A(\theta)^2 - B(\theta)^2]^{3/2}} \right) \quad (102)$$

for  $\theta$  outside the rescattering interval. As we observe in the latter case the result is a non-integrable function of  $\theta$  at points  $\theta_{min}$  and  $\theta_{max}$ .

To overcome this difficulty we have to remember that in reality the double pole at  $A - B \cos \phi$  is split into two close poles when one takes into account the small nuclear momenta neglected in (102). Thus in the vicinity of, say,  $\theta_{min}$  the integrand in (96)

$$Y(\theta) = \frac{1}{(1 - \cos \theta)^2} \int d\phi \text{Re } X_r(\theta\phi) \quad (103)$$

will have a singularity structure

$$Y(\theta) = Y_r(\theta) + \frac{1}{\alpha} \left( \frac{c}{\sqrt{\theta_{min} - \theta}} - \frac{c + c_1 \alpha}{\sqrt{\theta_{min} + t\alpha - \theta}} \right), \quad (104)$$

with  $Y_r$  a regular function and  $\alpha \ll 1$  proportional to the difference  $(\mathbf{q}, \mathbf{k}_1 - \mathbf{k}'_1)$ . In the limit  $\alpha \rightarrow 0$  we obtain from (104)

$$Y(\theta)_{\alpha \rightarrow 0} = Y_r(\theta) + \frac{\eta}{\sqrt{\theta_{min} - \theta}} + \frac{\zeta}{(\theta_{min} - \theta)^{3/2}}, \quad (105)$$

where

$$\eta = a - c_1, \quad \zeta = ct/2,$$

with a non-integrable singularity. However, correctly integrated, (104) has a finite limit at  $\alpha \rightarrow 0$  due to the dependence on  $\alpha$  of the limits of integration. Indeed one trivially finds in this limit

$$\int_{\theta_0}^{\theta_{min}} Y(\theta) d\theta = \int_{\theta_0}^{\theta_{min}} Y_r(\theta) d\theta + 2\eta \sqrt{\theta_{min} - \theta_0} - \frac{2\zeta}{\sqrt{\theta_{min} - \theta_0}}. \quad (106)$$

Quite a similar formula is obtained for the integral over the interval  $\theta_{max} < \theta < \theta_1$  with the substitution  $\theta_{min} - \theta_0 \rightarrow \theta_1 - \theta_{max}$  and of course different values for  $\eta$  and  $\zeta$ .

In principle the regularization functions  $r_{1,2}(\theta)$  and numbers  $\eta$  and  $\zeta$  for the two singular points in  $\theta$  can be obtained analytically. However the resulting expressions are very cumbersome, so that in practice we obtained them by studying numerically the corresponding singular behaviour.

An additional difficulty consists in that the lower singular point  $\theta = \theta_{min}$  for values of  $x_1$  close to unity turns out to be quite small and so very close to the point  $\theta = 0$  at which function  $Y_r$  acquires a singularity due to subtraction. To solve this problem we divide the interval  $[0, \theta_{min}]$  into two  $[0, \theta_0] + [\theta_0, \theta_{min}]$  and apply the regularization (106) only in the 2nd interval. As a result the integrations over these two intervals give large numbers cancelling each other, which imposes very stringent requirements on the numerical precision.

## 10 References

1. D.I.Blokhintzev, JETP **33** (1957) 1295.
2. I.A.Schmidt and R.Blankenbecler, Phys. Rev.**D 15** (1977) 3321; **D 16** (1977) 1318
3. L.L.Frankfurt and M.I.Strikman, Phys. Rep. **76** (1981) 215
4. A.V.Efremov, Yad. Fiz. **24** (1976) 1208;
- V.V.Burov, V.K.Lukianov and A.I.Titov, Phys. Lett. **B67** (1977) 46;
- A.V.Efremov, A.B.Kaidalov, V.T.Kim, G.I.Lykasov and N.V.Slavin, Yad. Fiz. **47** (1988) 1364.
5. M.I.Gorenshtein, G.M.Zinoviev and V.P.Shelest, Yad. Fiz. **26** (1977) 788.
6. L.A.Kondratiuk and V.B.Kopeliovich, JETP Lett. **21** (1975) 40;
- V.B.Kopeliovich, JETP Lett. **23** (1976) 313, Phys. Rep. **139** (1986) 51;
- M.A.Braun and V.V.Vechernin, Sov. J. Nucl. Phys. **25** (1977) 676, **28** (1978) 753.
7. M.A.Braun and V.V.Vechernin, J.Phys. **G 19** (1993) 517, 531
8. L.L.Frankfurt, M.I.Strikman, D.B.day and M.Sargsyan, Phys. rev. **C 48** (1993) 2451.
9. C.Bochna *et al.*, Phys. Rev. Lett. **81** (1998) 4576.
10. S.J.Brodsky and J.R.Hiller, Phys. Rev. **C 28** (1983) 475.
11. J.Gao *et al.*, Phys. Rev. Lett. **84** (2000) 3265.

## 11 Figure captions

Fig. 1. Diagrams illustrating different mechanisms of cumulative production: spetator (a), direct (b), compressed tube plus rescattering (c and d).

Fig. 2. Cumulative (solid line) and rescattering (dashed line) kinematical regions in the backward hemisphere at 6 GeV.

Fig. 3. Effective internucleon momentum space potential as extracted from the photo-production data [ 9 ].

Fig. 4 Nuclear coefficients  $f_0$  and  $c_0$ .

Fig. 5. Inclusive nucleon leptonproduction cross-sections on Cu at the incident energy 6 GeV in the backward hemisphere.

Fig. 6. Same as Fig. 5 on the Pb target.

Fig. 7. Double differential cross-sections in  $\mathbf{p}_1$  and  $Q^2$  for nucleon leptonproduction on Pb at the incident energy 6 GeV, emission angle  $\theta_1 = 90^\circ$  and  $Q^2 = 1 \text{ (GeV/c)}^2$ .

Fig. 8. Same as Fig. 8 at  $\theta_1 = 180^\circ$  and  $Q^2 = 1 \text{ (GeV/c)}^2$ .

Fig. 9. Same as Fig. 8 at  $\theta_1 = 90^\circ$  and  $Q^2 = 4 \text{ (GeV/c)}^2$ .

Fig. 10. Same as Fig. 8 at  $\theta_1 = 180^\circ$  and  $Q^2 = 4 \text{ (GeV/c)}^2$ .

Fig. 11. Double inclusive cross-section for the reaction  $e + {}^{16}\text{O} \rightarrow e'(p_e) + N(p_1) + X$  at  $E = 2.4$  GeV,  $Q^2 = 0.8$  (GeV/c) $^2$  and  $q_0 = 0.439$  GeV for the nucleons ejected into the backward hemisphere. Positive  $p_{miss} = |\mathbf{q} - \mathbf{p}_1|$  correspond to  $\phi_1 = 180^\circ$ , negative  $p_{miss}$  to  $\phi_1 = 0$ . The lower curve was obtained with an energy independent internucleon potential, the upper curve with a vector-like potential. Experimental points are from [ 11 ]. Lower (upper) points correspond to the  $1p_{1/2}$  ( $1p_{3/2}$ ) nuclear level.

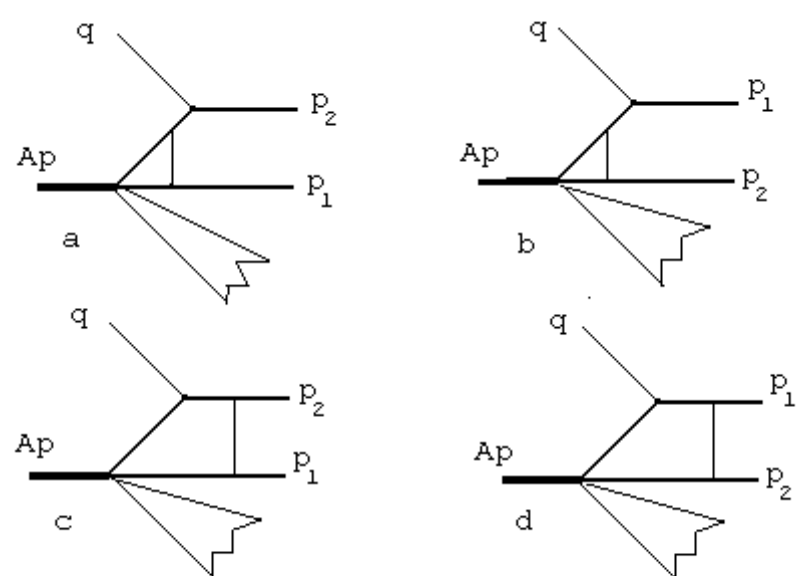


Fig.1

